Lab on a Chip

TECHNICAL INNOVATION

View Article Online
View Journal

Cite this: DOI: 10.1039/c5lc01536g

Hybrid PDMS/glass microfluidics for high resolution imaging and application to sub-wavelength particle trapping†

Mario Tonin,* Nicolas Descharmes and Romuald Houdré

Received 15th December 2015,
Accepted 22nd December 2015

DOI: 10.1039/c5lc01536g

www.rsc.org/loc

We demonstrate the fabrication of a hybrid PDMS/glass microfluidic layer that can be placed on top of non-transparent samples and allows high-resolution optical microscopy through it. The layer mimics a glass coverslip to limit optical aberrations and can be applied on the sample without the use of permanent bonding. The bonding strength can withstand to hold up to 7 bars of injected pressure in the channel without leaking or breaking. We show that this process is compatible with multilayer soft lithography for the implementation of flexible valves. The benefits of this application is illustrated by optically trapping sub-wavelength particles and manipulate them around photonic nano-structures. Among others, we achieve close to diffraction limited imaging through the microfluidic assembly, full control on the flow with no dynamical deformations of the membrane and a 20-fold improvement on the stiffness of the trap at equivalent trapping power.

Recent developments in microfluidics show an important trend in the use of polymers and thermoplastics instead of materials such as glass. Polydimethylsiloxane (PDMS) especially holds a privileged role in microfluidics because of several advantages compared to glass and other polymers. First, it is flexible and easy to fabricate by soft lithography.[1] It can be bonded permanently to PDMS or flat surfaces like glass or silicon by oxygen plasma activation. It can also be bonded temporarily by simple conformal contact thanks to van der Waals (VdW) forces, which form a water-tight seal between two flat surfaces. Second, PDMS is biocompatible and rather inexpensive.[2–5] It is common to use PDMS to fabricate channels for the immersion of nanostructure for sensing applications, such as ring resonators and photonic crystals.[6–9] Unfortunately, PDMS also has some limitations,[10] in particular when considering high-resolution imaging.

In most silicon-based structures, the sample is opaque to visible light. Thus, the imaging has to be done through the microfluidic layer. This also applies to any other opaque samples, like metallic substrates. Mostly two options have been investigated so far. The first option is to use a transparent PDMS microfluidic layer on top of the silicon sample. Another option would be to use a bonded SU8 microfluidic layer.[13] This option is limited to the fabrication of simple, externally driven microfluidic channels and doesn't allow a precise control of the flow within the micro-channels. Precise control of the flow in microfluidic membranes is generally performed with flexible valves. It is necessary when working with small objects in the solution injected in the micro-chanels.

High resolution imaging is generally performed with immersion objectives, which have very strict operational conditions for limiting aberrations. In particular, the refractive index n_D and the thickness t of the glass coverslip used have to be as close as possible to the predefined values used to design the objective (typically n_D = 1.523 and t = 170 μm). Because of this, large membranes in PDMS (n_D around 1.43) or SU8 (n_D around 1.6) prevent working in high resolution. When using this materials as the cover layer, it is possible to reach a thickness close to 170 μm but the refractive index mismatch is still an issue.

In a previous work,[11,12] the use of a thin microfluidic PDMS layer has been demonstrated. While this approach works, the overall optical quality is still rather poor. Additionally, the small thickness of the PDMS layer introduces some side effects that degrades the general performance of the membrane. For example, diffusion of chemicals from the synthetic immersion oil through the PDMS polymer matrix[14]

Institut de Physique de la Matière Condensée, École Polytechnique Fédérale de Lausanne, Lausanne, Switzerland. E-mail: romuald.houdre@epfl.ch; Tel: +41 2169 35855

† Electronic supplementary information (ESI) available: Video of working valves with flow inversion viewed with fluorescent nanoparticles, mag 10×. Video of optical trapping inside the microfluidic channel of 500 nm polystyrene particles with classical tweezers and integrated resonant cavities, image of the sample with oil bubbles appearing in the microfluidic channel of a thin PDMS-only membrane, image of the alignment of the membrane on photonic crystal structures, images of the photonic crystals seen through the PDMS-only membrane and a hybrid glass/PDMS membrane. Image of the resolution target seen through PDMS-only microfluidics and through the hybrid membrane. See DOI: 10.1039/c5lc01536g

has been observed. Those chemicals can migrate to the channels and form viscous bubbles that can clog the microfluidic network (see additional figure). An oscillating residual flow inside the microfluidic channel when the valves were closed was also observed. This effect was attributed to the dynamic deformation of the structure. Finally, permanent bonding of the PDMS layer onto the silicon sample was required to withhold the injected pressure, even for a few 0.1 bar.

In this work, we introduce an hybrid glass and PDMS microfluidic membrane consisting of a 30 μm PDMS layer and a 145 μm microstructured glass layer. This membrane is positioned on top of the silicon nanostructured sample of interest. The glass layer has several benefits. First, its refractive index is matched to that of immersion oil objective specification, hereby reducing the spherical aberrations of the system. Second, the glass layer isolates the PDMS from the immersion oil. This prevents the formation of bubbles in the microfluidics channels. Third, the rigidity of the glass reduces the deformations of the membrane, which improves the stability of the flow in the micro channels. Last, since the layer is not bonded permanently, it can be removed without damaging the sample. This opens the door for possible replacement of the membrane if required.

1 Material and methods

The microfluidic layer is composed of two non-permanently bonded layers. A thin 30 μm flexible PDMS layer that acts as the fluidic transport layer and a thick 145 μm layer of borosilicate glass D263T acting as the control layer. The fabrication steps are shown in Fig. 1 and the final device in Fig. 2.

1.1 PDMS fluidic transport layer

The PDMS fluidic transport layer is fabricated by soft lithography. A silicon wafer is spin coated with AZ 9260 in order to have a thickness of 10 μm, which is the thickness of the desired microfluidic channel. The width of the channel is 200 μm. The wafer is baked at 115 °C for 3 min 20 s. The design of the channel is etched on a chromium mask by direct laser writing and transferred onto AZ 9260 photoresist after UV light exposure in a Süss Microtech MJB3 UV400 mask aligner for 80 s. The AZ 9260 is developed in AZ 400 1 : 4 for 6 minutes and rinsed in water. The edges of the channel are rounded by heating the mould at 150 °C for 90 minutes. The rounded channels are easier to close with flexible valves. The mould can generally be used 20–30 times before showing signs of degradation. A passivation layer is generated on the surface of the mould by placing it in a desiccator with a few drops of trimethylchlorosilane (TMCS). This helps releasing the PDMS layer after polymerization and is a critical step since the PDMS layer is very thin and fragile. The PDMS is mixed with a curing agent at a ratio of 10 : 1 and centrifuged at 2200 rpm for 2 minutes to eliminate bubbles. The PDMS is then poured on the mould and spun at 2000 rpm for 40 seconds to reach a thickness of 30 μm. The PDMS is then baked at 80 °C for 50 minutes. The resulting layer needs to be as flat as possible, without any air bubbles or dust on the surface.

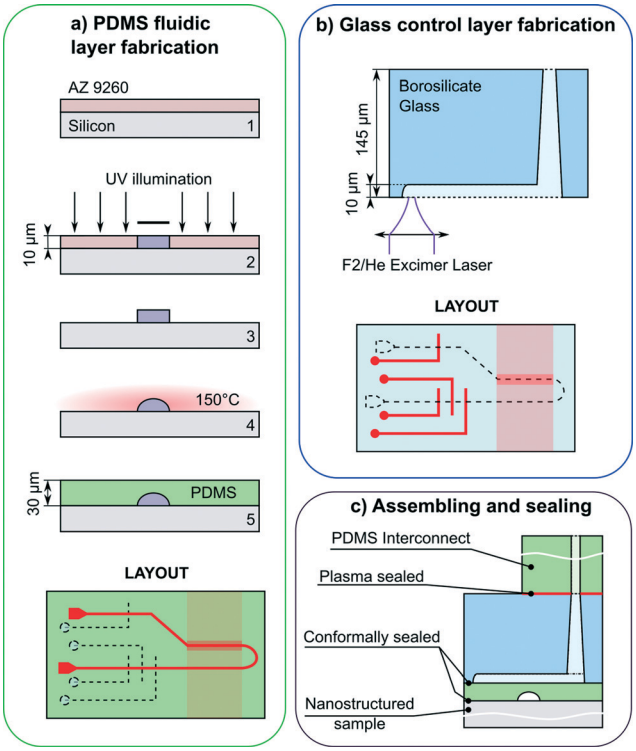

Fig. 1 a) Details of the fabrication process for the PDMS fluidic layer. The layout shows the design for the chip, where the red line is the fluidic channel. The dashed lines indicate the positions for the channels on the control layer. The shaded red area is the nanostructure area, with the photonic crystals being just underneath the fluidic channel. b) Details of the fabrication of the glass control layer. c) Final structure of the sample.

1.2 Glass control microfluidics

The glass layer is fabricated through excimer laser etching of a 145 μm thick borosilicate D263T glass wafers cut to the dimensions of the microfluidic layer (10 × 30 mm). The excimer laser is operating at 193 nm. It is capable of creating channels at the surface of the glass down to a resolution of 10 μm. It is also capable of creating through holes in the glass layer. The roughness of the channel is controlled with the shape, the fluence, the scanning speed and the pulse rate of the laser beam. In our case, the fluence of the laser was set at 2.7 J cm^{-2} and was able to etch 48 nm of glass per pulse. The glass layer is then cleaned with an ultrasonic bath before the assembly.

1.3 Assembling and interconnect

The assembly is performed manually under binoculars. The PDMS layer is cut and peeled off the mould. Holes for the injection of the fluid are punched through the PDMS layer. The PDMS layer is then positioned and aligned on the glass layer so that the injection holes in the PDMS and in the glass coincide. The relative position of the two layers is important so

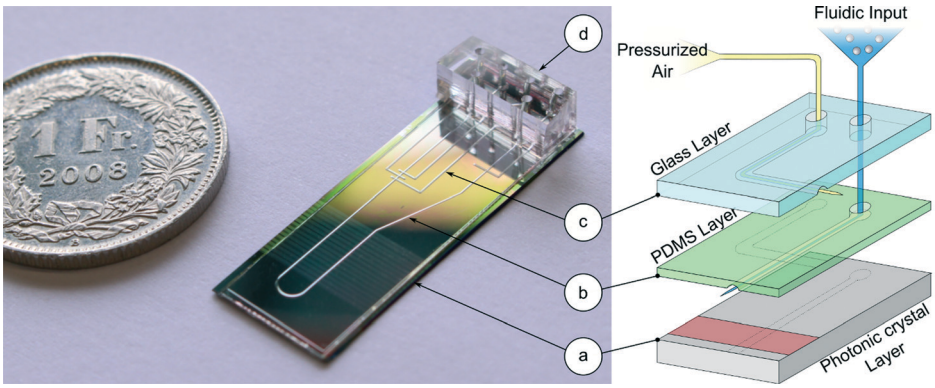

Fig. 2 Image of the final device with the microfluidic layer. a) Silicon sample with photonic crystal and waveguide in the red area. b) PDMS layer for the fluid and nanoparticles. The fluidic microchannel is the channel with a U shape. c) Glass layer where the control channels are injected with pressurized air. d) PDMS interconnect block.

that the fluidic (in PDMS) and control (in glass) channels cross to realize Quake valves.[15] Manipulating the thin layer of PDMS can be difficult due to electrostatic effects. One method to make manipulation easier is to have a PDMS joist attached at the bottom of the membrane to rigidify it. This joist is then removed after alignment on the glass. There is no need for plasma activation when bonding the PDMS and the glass coverslip. The conformal contact between the two surfaces is sufficient to form a non-permanent seal that is watertight around the injection holes. The microfluidic assembly is rigid at this point and allows for precise manipulation. The PDMS/glass layer is then aligned on the structures, with the PDMS in contact to the nanostructured opaque substrate. This alignment might have to be precise depending of the structures of interest. In this case, the structures of interest consist of silicon photonic crystal membranes containing individual optical cavities (10 × 40 μm). Their fabrication on a SOI substrate is discussed elsewhere.[11] The dimensions of the individual membranes are 10 × 40 μm, and should be completely immersed in the fluidic channel. Alignment tolerances are therefore around 50 μm on each side. A view of the aligned channel can be seen in the additional content.

The connection to the external control for the microfluidics is done through an interconnect. The later is a piece of PDMS that is permanently bonded on top of the glass after plasma activation. It is big enough to hold tubes and inject water and air in the fluidic and control channels respectively. Plasma bonding is required because of the forces and torque that occurs on the interconnect through the tubes. After plasma bonding, the sample is left in an oven overnight at 80 °C.

2 Results

2.1 Optical advantages: near-diffraction limited imaging

Photonic crystals imaged through the hybrid microfluidics show an increasing amount of detail as can be seen in the additional content. For a full PDMS layer of 160 μm, the effect of spherical aberration are evidenced in the inserts of Fig. 3 where a NSB 1010A type microscopy resolution target is imaged through a PDMS layer. A larger image of the target is in the supplementary content. The cut-off for this layer is 1400 lines per mm, which correspond to a resolution of 700 nm. On the other hand, the same target imaged through the hybrid PDMS/glass layer has a cut-off of 2200 lines per mm corresponding to a resolution of 450 nm, which is close to the theoretical resolution limit of $1.22\lambda/NA$ = 435 nm for imaging at a wavelength of 500 nm.

This improvement can also be observed in Fig. 4 showing an image of a fluorescent particle with a diameter of 500 nm. The top image is done through the 170 μm PDMS-only layer while the bottom image is done through the hybrid layer. The same immersion objective is used in both cases. The image of the particle obtained through the PDMS-only microfluidics as a full width at half maximum (FWHM) of 890 nm. When imaging the same kind of particle with the hybrid PDMS/glass microfluidic, the FWHM is reduced to 590 nm. These particles have a fluorescent emission around 600 nm. A Zemax simulation shows that the diffraction-limited FWHM of such particles is 500 nm.

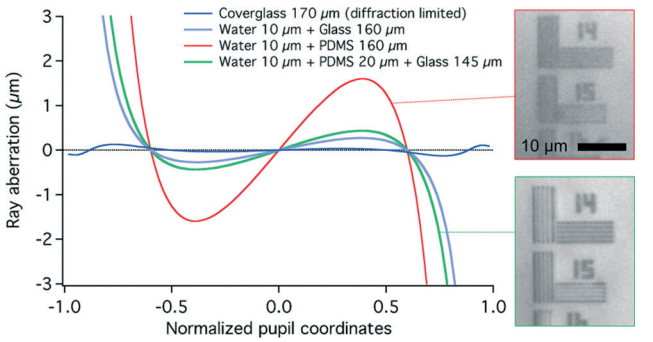

Fig. 3 Aberration calculated for several micfrofluidics layer. Inserts: Images from the adapted NBS1010A microscopy resolution targets. Cut-off frequency for the full PDMS layer is at 1400 lines per mm whereas the cut-off is at 2200 lines per mm for the hybridmicrofluidics. Illumination wavelength is 520 nm.

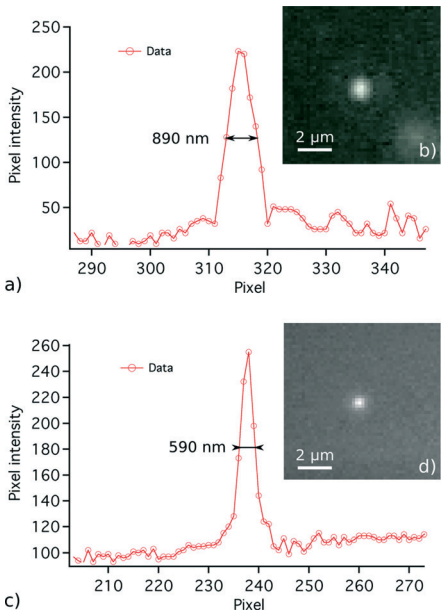

Fig. 4 a) Intensity profile of the 500 nm diameter fluorescent particle imaged through the PDMS-only microfluidic layer visible in picture b). c) Intensity profile of the 500 nm diameter fluorescent particle imaged through the hybrid PDMS/glass microfluidic layer visible in picture d).

The effect of the composition of the microfluidic layer on the aberration have been computed with Zemax in Fig. 3. This figure represents the deviation of the focus spot along the optical axis for a collimated beam coming from a position in the pupil plane. One can see that the aberration curve for the glass coverslip is close to the zero line of the plot, which means that the imaging is well corrected in this case. On the contrary, the red curve corresponding to the PDMS-only microfluidic presents large fluctuations, which means that strong spherical aberrations hinder the optical quality of the image. The hybrid layer, where the image is done through 145 μm of glass, 20 μm of PDMS and 10 μm of water (thickness of the fluidic channel filled with water), lies in between. In this case, the aberration line is very similar to the case of a glass coverslip with a thin layer of water. This is a clear improvement on the imaging quality, which is at the origin of the improved imaging quality of the hybrid membrane.

2.2 Mechanical properties

One of the main reason behind the introduction of the glass layer in the microfluidic assembly, besides the near diffraction limited imaging, is the protection against oil infiltration in the channels and the stabilization of the residual flow observed while stoping the flow in the channel. As expected, the infiltration of oil is prevented and the residual flow is stabilized. Additionally, plasma bonding of the microfluidic structure was not required. The membrane is capable of withholding the pressure needed to actuate the Quake valves. This is a surprising result because non-permanent bonded PDMS cannot usually withhold as much pressure as permanently bonded structures (this limit is usually 0.35 bar (ref. 16)). On the contrary here, the hybrid membrane show greatly improved resistance to input pressure, up to the 7 bars reachable in our setup. This correspond to an improvement of at least 20 times. This can be understood from the rigidity of the glass that is redistributing and supporting most of the stress in the hybrid membrane.

This can be simulated by looking at the von Mises (VM) stress, which is related to the deviatoric strain in the material. The VM stress is generally used to represent the contribution of the stress deforming the material under study. Simulations in a full PDMS microfluidic layer show that the VM stress is mostly located at the contact point between the silicon and the PDMS at the edges of the channel (Fig. 5b). For 0.35 bar injected inside the microfluidic channel, the maximum stress simulated reaches 730 kPa. The hybrid membrane on the other hand distributes part of the stress in the glass layer (Fig. 5d). For 0.35 bar in the channel, the maximum stress in the glass at 65 kPa is well below the yield stress for borosilicate (7 MPa). In the PDMS layer, the maximum stress is still at the same contact point as before, for a value of 145 kPa, which is 6 times less than for the full PDMS layer. Moreover, it is interesting to compare the direction and the displacement of the layer in both types of membranes. The full PDMS membrane shows strong displacement perpendicular to the surface above and close to the microfluidic channel (Fig. 5a). The VdW adhesive forces primarily will counter this type of displacement. The displacement of the hybrid membrane differs as larger displacements exist inside the PDMS layer and are angled with the silicon surface at the edges of the channel. The displacement at the centre of the channel is still vertical but 25 times less than with the full PDMS layer (Fig. 5b) when simulated for 0.35 bar of pressure. Simulations with 7 bars in the hybrid membrane show that the VM stress rises to 3 MPa in the PDMS at the same contact point as before. The stress in the glass layer is 1.5 MPa, which is still bellow the breaking point. This ability to withstand pressure from inside the channel doesn't prevent the removal of the microfluidic layer. The layer can be removed from the substrate by applying a torque between the PDMS layer and the glass layer with a tool such as a scalpel. With this technique, the same photonic crystal sample has been used with a different hybrid membranes up to ten times with no apparent damages to the silicon structures.

3 Application to optical trapping and integrated photonic crystal cavities structures

The increase of the resolution has significant impacts, for instance when optically trapping a particle inside the channel using a focused laser beam going through the microscope objective and through the microfluidic layer.[11,12] Trapping a polystyrene sphere of 500 nm diameter is more efficient with the hybrid microfluidic than with the PDMS-only

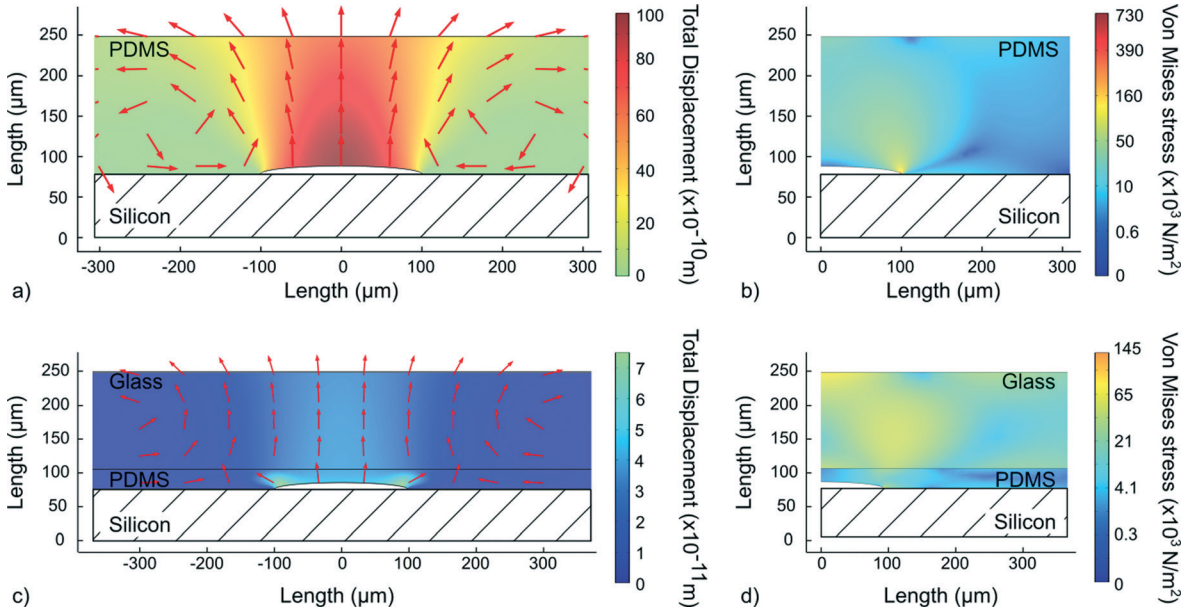

Fig. 5 a) FEM simulation of the displacement of the PDMS layer under a pressure of 0.35 bar inside the fluidic channel. The arrow length is normalized and only indicates the direction of the displacement. The surface between the PDMS and the silicon is fixed. b) FEM simulation of the von Mises stress inside the PDMS layer (quadratic scaling). c) FEM simulation of the displacement of the hybrid PDMS and glass layer with normalized arrows under 0.35 bar of pressure. The magnitude of the displacement is more than 10 times less than with the full PDMS microfluidics for the same applied pressure. d) FEM simulation of the von Mises stress inside the PDMS and glass layers (non linear scaling). The magnitude of the stress is 6 times less than with the full PDMS microfluidics.

microfluidic. This is demonstrated when plotting the centroid of the position of the center of emission of a nanoparticle of 500 nm in polystyrene trapped with the same amount of power in both case in Fig. 6. From this data it is possible to measure the trap stiffness k of the optical tweezer in both cases, using the equipartition theorem: $k = k_B T/\sigma^2$ where σ is the standard deviation. We find that the trap stiffness of the optical tweezer through the hybrid layer is almost 20 times larger than with the PDMS-only microfluidic. This in turns allows trapping spheres that are smaller in size with the same power.

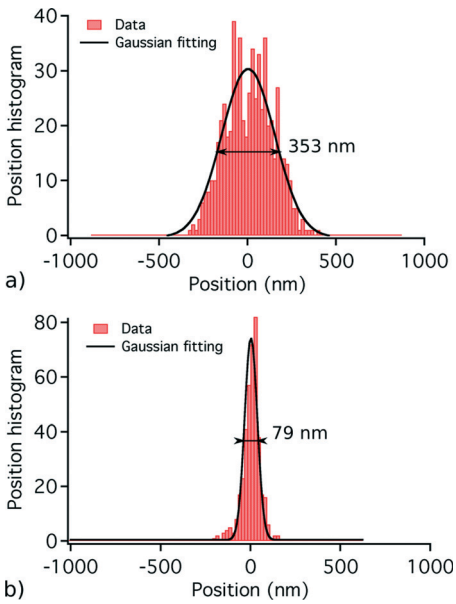

Fig. 6 a) Histogram of the centroid of the position of trapped 500 nm polystyrene particles within the PDMS-only microfluidic layer. b) Histogram of the centroid of the position of trapped 500 nm polystyrene particles within the hybrid PDMS/glass microfluidic. The laser used to trap the particules in a) and b) is a Ti:Sapph operating at 900 nm, with the same output power of 100 mW in both cases.

As an illustration it was used to bring particles close to photonic nanostructures for integrated optical trapping using hollow photonic crystal cavities.[11,12] The results in these papers were obtained using a thin PDMS-only microfluidic membrane. The control of the flow inside the microfluidic channel is important for this application, since the measurements have to be in a stable environment. For the experiments, the flow was completely stopped so that the particles can be in Brownian motion with no external drift. The other function of the layer is to provide good optical qualities in order to record the motion of the trapped nanoparticles using interferometry.[17] For this method, a laser beam is focused on the particle with an oil immersion objective. These measurements have the best lateral resolution when the focus spot of the detection laser is as small as possible.[18] Moreover, classical optical trapping of nanoparticles can be performed with a beam passing through the membrane in order to position them in the photonic crystal cavities, as demonstrated in the video in the additional material. More complex microfluidic channels can be realized inside the PDMS layer, with the corresponding valves, or other fluidic channels in the glass.

4 Conclusion

We present a microfluidic membrane that can be laid on top of opaque samples. Because of its composition, it can be used to make high resolution images of structures embedded in the microfluidic channel through the membrane. Thanks to this hybrid microfluidic structure, the resolution of our experiments is increased, which enable us to track the Brownian motion more efficiently. Moreover, optical trapping performed by an external laser through the microfluidics gives a trap with a stiffness 20 times larger in our hybrid design compared to the design with PDMS layers only. Finally, we also show the ability to integrate Quake valves in this design in order to control the flow in the fluidic channel and is very resistant to injected pressure up to 7 bar without permanent bonding to the sample required.

Acknowledgements

The authors acknowledge the financial support from the Swiss National Science Foundation Project No. 200020_153538. The authors thank H. P. Herzig and T. Scharf for the Zemax simulations, and M. Sabry for helpful discussions.

References

1 J. C. Mcdonald, D. C. Duffy, J. R. Anderson and D. T. Chiu, *Electrophoresis*, 2000, **21**, 27–40.
2 H. Becker and L. E. Locascio, *Talanta*, 2002, **56**, 267–287.
3 G. M. Whitesides, *Nature*, 2006, **442**, 368–373.
4 E. Berthier, E. W. K. Young and D. Beebe, *Lab Chip*, 2012, **12**, 1224.
5 T. Squires, *Rev. Mod. Phys.*, 2005, **77**, 977–1026.
6 J. E. Baker, R. Sriram and B. L. Miller, *Lab Chip*, 2015, **15**, 971–990.
7 Z. Wang, H. Yan, S. Chakravarty, H. Subbaraman, X. Xu, D. Fan, A. X. Wang and R. T. Chen, *Opt. Lett.*, 2015, **40**, 1563–1566.
8 M. G. Scullion, Y. Arita, T. F. Krauss and K. Dholakia, *Optica*, 2015, **2**, 816–821.
9 O. Krupin, C. Wang and P. Berini, *Lab Chip*, 2015, **15**, 4156–4165.
10 R. Mukhopadhyay, *Anal. Chem.*, 2007, 3249–3253.
11 M. Scullion, A. D. Falco and T. Krauss, *Biosens. Bioelectron.*, 2011, **27**, 101–105.
12 N. Descharmes, U. P. Dharanipathy, Z. Diao, M. Tonin and R. Houdré, *Lab Chip*, 2013, **13**, 3268–3274.
13 N. Descharmes, U. P. Dharanipathy, Z. Diao, M. Tonin and R. Houdré, *Phys. Rev. Lett.*, 2013, **110**, 123601.
14 J. Ng Lee, C. Park and G. M. Whitesides, *Anal. Chem.*, 2003, **75**, 6544–6554.
15 M. A. Unger, H.-P. Chou, T. Thorsen, A. Scherer and S. R. Quake, *Science*, 2000, **288**, 113–116.
16 J. C. Mcdonald, M. L. Chabinyc, S. J. Metallo, J. R. Anderson, A. D. Stroock and G. M. Whitesides, *Anal. Chem.*, 2002, **74**, 1537–1545.
17 A. Pralle, M. Prummer, E.-L. Florin, E. Stelzer and J. Hörber, *Microsc. Res. Tech.*, 1999, **44**, 378–386.
18 A. Rohrbach and E. H. K. Stelzer, *J. Appl. Phys.*, 2002, **91**, 5474–5488.

